

This article was downloaded by: [Tomsk State University of Control Systems and Radio]

On: 19 February 2013, At: 14:24

Publisher: Taylor & Francis

Informa Ltd Registered in England and Wales Registered Number: 1072954  
Registered office: Mortimer House, 37-41 Mortimer Street, London W1T 3JH, UK



## Molecular Crystals and Liquid Crystals

Publication details, including instructions for authors and subscription information:

<http://www.tandfonline.com/loi/gmcl16>

### A Calorimetric Measurement of Phase Transformation Kinetics in Solid Octaphenylcyclotetrasiloxane: Evidence for Nucleation as the Rate Determining Process

George W. Smith<sup>a</sup>

<sup>a</sup> Physics Department, General Motors Research Laboratories, Warren, Michigan, 48090-9055

Version of record first published: 20 Apr 2011.

To cite this article: George W. Smith (1986): A Calorimetric Measurement of Phase Transformation Kinetics in Solid Octaphenylcyclotetrasiloxane: Evidence for Nucleation as the Rate Determining Process, *Molecular Crystals and Liquid Crystals*, 132:3-4, 385-410

To link to this article: <http://dx.doi.org/10.1080/00268948608079555>

PLEASE SCROLL DOWN FOR ARTICLE

Full terms and conditions of use: <http://www.tandfonline.com/page/terms-and-conditions>

This article may be used for research, teaching, and private study purposes. Any substantial or systematic reproduction, redistribution, reselling, loan, sub-licensing, systematic supply, or distribution in any form to anyone is expressly forbidden.

The publisher does not give any warranty express or implied or make any representation that the contents will be complete or accurate or up to date. The accuracy of any instructions, formulae, and drug doses should be independently verified with primary sources. The publisher shall not be liable for any loss, actions, claims, proceedings, demand, or costs or damages whatsoever or howsoever caused arising directly or indirectly in connection with or arising out of the use of this material.

# A Calorimetric Measurement of Phase Transformation Kinetics in Solid Octaphenylcyclotetrasiloxane: Evidence for Nucleation as the Rate Determining Process

GEORGE W. SMITH

*Physics Department, General Motors Research Laboratories,  
Warren, Michigan 48090-9055*

*(Received August 7, 1985)*

The kinetics of transformation from the metastable (at high temperature) solid 3-phase of octaphenylcyclotetrasiloxane to the stable 2-phase have been measured by a calorimetric technique. The results of the kinetic study and several related experiments are consistent with the view that nucleation is the rate determining process. Transformation time constants for large and small crystallites were found; the temperature dependence of each is in accord with the Turnbull-Fisher nucleation theory. From that theory  $\gamma$ , the interfacial energy between the 3- and 2-phases, has been found to be  $\sim 3$  ergs/cm<sup>2</sup>, an order of magnitude smaller than that for typical liquid-solid interfaces. A study of the dependence of the transformation kinetics on crystallite size suggests that the phase change is surface nucleated.

*Keywords: phase transitions, phase transformation kinetics, calorimetry, nucleation, solid-solid transitions*

## I. INTRODUCTION

Understanding the mechanisms and kinetics of nucleation and growth of condensed phases is important to a variety of phenomena: e.g.,

formation of mesophases (liquid crystals, carbonaceous mesophase<sup>1</sup>); solidification, condensation, and solid-solid phase transformations; and the formation of aerosols. Although kinetic models for nucleation and growth have been developed,<sup>2</sup> testing these models experimentally is often difficult because the transformation is frequently rapid. In particular, solid-solid phase transformations are incompletely understood.<sup>3,4</sup> In order to understand these phenomena it is important to study the rates<sup>3</sup> and mechanisms<sup>4</sup> of formation of solid nuclei.

An interesting and useful system in which to study the kinetics of phase transformations is pure solid octaphenylcyclotetrasiloxane [ $\text{SiO}(\text{C}_6\text{H}_5)_2$ ]<sub>4</sub> (abbreviated OPCTS), for which at least three phases are known.<sup>5</sup> The 3-phase (stable at room temperature) and the higher temperature 2-phase have been shown to be ordinary brittle crystalline phases.<sup>5</sup> X-ray crystallographic data for the 3- and 2-phases have been reported.<sup>6-9</sup> In 1975, Keyes and Daniels,<sup>10</sup> on the basis of a differential thermal analysis (DTA) study, suggested that the highest temperature 1-phase is a "plastic crystal" (or orientationally disordered crystal). The proposed plastic crystalline nature of the 1-phase was supported by calorimetric, optical and mechanical results;<sup>5</sup> a subsequent calorimetric study<sup>11</sup> was in substantial agreement with the results of Reference 5. X-ray diffraction,<sup>12</sup> nuclear magnetic resonance,<sup>13-15</sup> and quasi-elastic neutron scattering<sup>15</sup> investigations further supported the plastic-crystalline nature of the 1-phase.

In Reference 5 it was shown that the low-temperature 3-phase, under certain circumstances, will transform very slowly to the higher-temperature 2-phase even when superheated by more than 100 K. It was proposed that nucleation is the rate-controlling mechanism for this transformation from the metastable 3-phase to the stable 2-phase. Both calorimetric and microscopic evidence were cited to support this interpretation. In particular, the scan-rate dependence of differential scanning calorimetry (DSC) peaks were shown to obey a relationship based on a homogeneous nucleation model.

However, this previous work did not yield a direct measurement of the time dependence of the phase transformation. Rather, conclusions concerning the time dependence of the transformation were drawn from the scan-rate studies which were actually sensitive to the early, incubation stage of the nucleation process. In the present paper we report direct calorimetric measurements of the 3 → 2 transformation kinetics. We shall derive time constants for the phase transformation and show that they are consistent with the view that nucleation, rather than growth, controls the transformation kinetics.

## II. OPCTS GIBBS FUNCTION DIAGRAM AND $3 \rightarrow 2$ TRANSFORMATION

The phase behavior of pure OPCTS is best understood in terms of a schematic Gibbs function diagram (Figure 1). The 3-phase (stable below  $T_{32}$ , metastable above  $T_{32}$ ) can actually be observed for "virgin" samples<sup>†</sup> at temperatures well above  $T_{32} = 349.8$  K (76.6°C) and as high as  $T_{31} = 458.8$  K (185.6°C). The metastable 3-phase transforms to the 2-phase at a rate which increases as the temperature is raised from  $T_{32}$  to  $T_{31}$ . However, for a typical virgin sample (weighing  $\sim 4$  mg and containing several hundred crystallites), the transformation is sufficiently slow that some 3-phase can be preserved for a long time (tens of minutes to hours) all the way up to  $T_{31}$ . The probability that a  $3 \rightarrow 2$  transformation will occur is smaller for small crystallites (see Reference 5 and below) than for large crystallites. Since some  $3 \rightarrow 2$  transformation does occur with increasing tem-

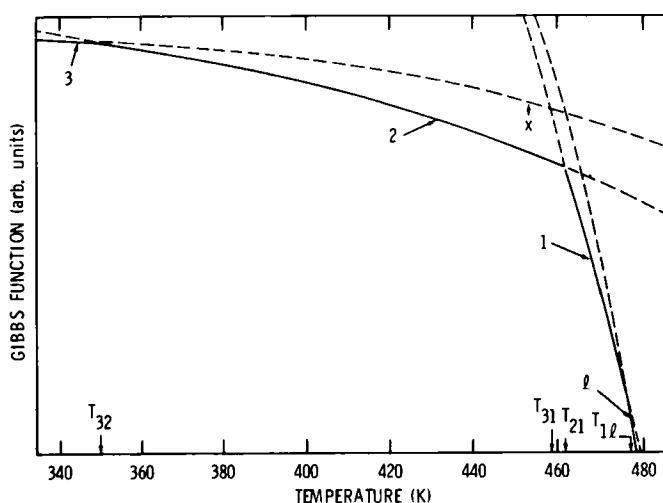


FIGURE 1 Schematic Gibbs function diagram for octaphenylcyclotetrasiloxane (OPCTS). 3, 2, 1 = solid phases;  $\ell$  = liquid;  $T_{32}$ ,  $T_{31}$ ,  $T_{21}$ ,  $T_{1\ell}$  = indicated transition temperatures;  $x$  = mole fraction of 3-phase converted to 2-phase (after Reference 5).

<sup>†</sup> Virgin samples were composed of high purity polycrystalline OPCTS as received from the supplier (see Section IV.A below). The material had been stored in a closed container at room temperature for several years, presumably ample time for stresses introduced during synthesis to relax.<sup>5</sup>

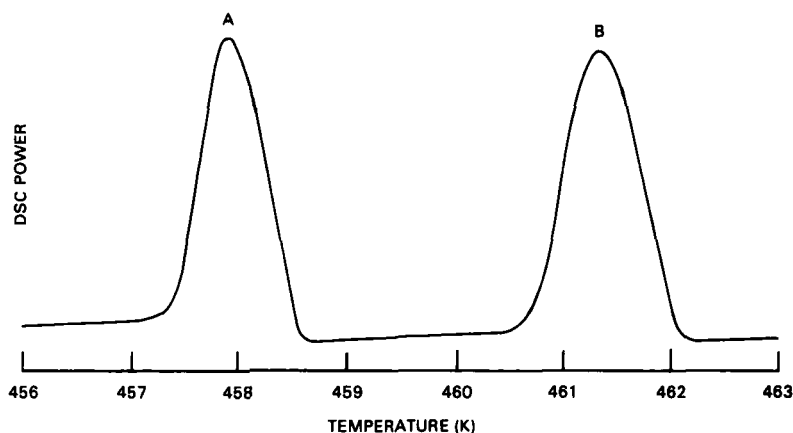


FIGURE 2 DSC scan showing the *A* and *B* peaks for a virgin OPCTS sample, at  $T_A$  and  $T_B$ , respectively (after Reference 5).

perature, both 3- and 2-phases are present as the temperature approaches  $T_{31}$ . As a consequence, DSC scans through the temperature range of the  $3 \rightarrow 1$  and  $2 \rightarrow 1$  transitions show two endotherms, designated the *A* peak (at  $T_{31}$ ) and *B* peak (at  $T_{21}$ ) (see Figure 2). The enthalpies of the two peaks,  $L_A$  and  $L_B$  are sensitive to the rate of temperature scan,<sup>5</sup> reflecting differences in mole fraction  $x$  of 3-phase which has transformed to 2-phase during the time of scan up to  $T_{31}$ . As we shall see, the values of  $L_A$  and  $L_B$  also depend on the length of time a virgin sample is held at a temperature just below  $T_{31}$ .

There are essentially two reasons why metastable 3-phase can be preserved at temperatures as high as  $T_{31}$  (more than 100 K above  $T_{32}$ ) in a virgin sample: (1) The driving force for transformation<sup>16</sup> is low; that is,  $\Delta G_{32}$ , the Gibbs function difference between the 3- and 2-phases is rather small† over the entire temperature from  $T_{32}$  to  $T_{31}$ . (A small value of  $\Delta G_{32}$  might also be reflected in a small value of  $\gamma$ , the interfacial energy between the two phases.) (2) The density of nucleation sites in each of the several hundred crystallites of a typical virgin sample is sufficiently small that the formation of the stable 2-phase is very slow.

The contention that lack of nuclei (rather than slow growth) is largely responsible for the preservation of metastable 3-phase at high temperatures in a virgin sample is borne out by the facts that the

† In Figure 1 the relative difference of the Gibbs function for the two phases is considerably exaggerated.

probability of  $3 \rightarrow 2$  transformation is lower in a small crystallite of a virgin sample than in a large one, and that all material in a given crystallite transforms almost simultaneously.<sup>5</sup> This view that nucleation controls the transformation rate is further supported by the contrasting behavior for non-virgin OPCTS samples. Formation of the 2-phase above  $T_{32}$  is much enhanced in samples which have been heat treated to temperatures above  $T_{31}$  (see Reference 5), in samples consisting of large crystallites, in less pure samples, and in ground samples (see below). Heat treatment, large crystal size, impurities, and grinding all tend to increase the number of nucleation sites which would greatly accelerate formation of the stable phase.<sup>17</sup>

In Reference 5 it was shown that  $x$ , the mole fraction of 3-phase which had transformed to 2-phase could be determined from  $L_A$  and  $L_B$ , using the following relations:

$$L_A = (1 - x) L_{31} \quad (1)$$

and

$$L_B = x L_{21} \quad (2)$$

where  $L_{31}$  and  $L_{21}$  are the enthalpies of the  $3 \rightarrow 1$  and  $2 \rightarrow 1$  transitions.<sup>†</sup>

In that earlier work the scan-rate dependence of  $x$  determined from  $L_A$  and  $L_B$  was used to obtain information about the transformation kinetics. We felt, however, that a more direct measurement of the time-dependence of  $x$  was needed in order to determine whether nucleation was indeed the controlling factor. Before we turn to the kinetic experiments in which we determined  $x$  as a function of  $t$ , let us consider in Section III two experiments designed to introduce nucleation sites as a test of our contention that nucleation governs the  $3 \rightarrow 2$  transformation.

### III. EXPERIMENTS OF IMPURE AND GROUND OPCTS

In Reference 5, it was shown that for pure OPCTS samples which had been previously heated above  $T_{31}$  (or above the melting point) the 3-phase was not preserved through the region of metastability

<sup>†</sup> In Reference 5,  $L_A$  and  $L_B$  were determined by hand integration techniques, yielding  $L_{31} = 47.3$  kJ/mol and  $L_{21} = 43.8$  kJ/mol. More precise computer integration used in the present work gave values  $\sim 5\%$  smaller (44.3 and 42.7 kJ/mol respectively).

( $T_{32} < T < T_{31}$ ). Hence, heat treated samples exhibited a very large  $B$  peak (at  $T_{21}$ ) and essentially no  $A$  peak. It was argued<sup>5</sup> that strains or defects introduced by warming and cooling through the phase transition (or the melting point in some cases) acted as nucleation sites for rapid  $3 \rightarrow 2$  transformation during subsequent DSC runs.<sup>17</sup>

To test this concept further we have studied OPCTS samples into which nucleation sites had presumably been introduced. Two types of samples were investigated: OPCTS of apparently lower purity and material subjected to varying degrees of grinding.

### A. Impure samples

The "impure" sample was obtained from a different source from that of Reference 5. Since its melting point was about 1 K lower, we felt that its purity was less than the  $99.97 \pm 0.02\%$  determined calorimetrically for the high purity sample. The presence of impurity, it was believed, would introduce nucleation sites, although the influence of other sample preparation differences could not be ruled out. At any rate in the case of less pure samples, as anticipated, we did not observe the DSC phenomenon associated with preservation of 3-phase at temperatures in the metastable region (the presence of both  $A$  and  $B$  peaks for a virgin sample). Thus, only a  $B$  peak was observed.

### B. Ground samples

Several samples of the high purity virgin OPCTS were subjected to grinding in a Wig-L-Bug<sup>18</sup> for times ranging from  $\sim 1$  to 90 seconds, a process which should introduce strains and defects (and perhaps impurities) as well as enhanced surface nucleation sites. The influence of grinding on  $L_A$  and  $L_B$  and on  $L_m$ , the melting enthalpy (all measured at the same scan rate, 2.5 K/min) is shown in Figure 3. The enhancement of  $L_B$  and the reduction in  $L_A$  by grinding for only a few seconds indicates from Equations (1) and (2) that  $x$  was greatly enhanced. This experiment is consistent with the view that grinding introduced nucleation sites which markedly increased the  $3 \rightarrow 2$  transformation rate. The influence of grinding on the temperatures of the  $A$ ,  $B$ , and melting peaks is shown in Figure 4. Although  $T_m$  and  $T_A$  were affected by grinding,  $T_B$  was not.<sup>†</sup>

The experiments with impure and ground OPCTS are in accord

<sup>†</sup> The reduction in  $T_m$  may be due to the introduction of impurities; the decrease in  $T_A$  is probably due to the fact that peak temperature in DSC experiments approaches the temperature of peak onset as peak area decreases.



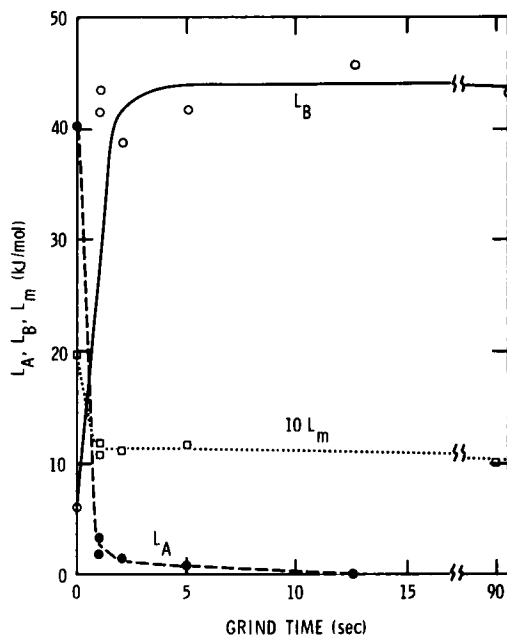


FIGURE 3 Influence of grind time on  $L_A$ ,  $L_B$ , and  $L_m$ , the transition enthalpies for the A, B, and melting peaks for OPCTS.

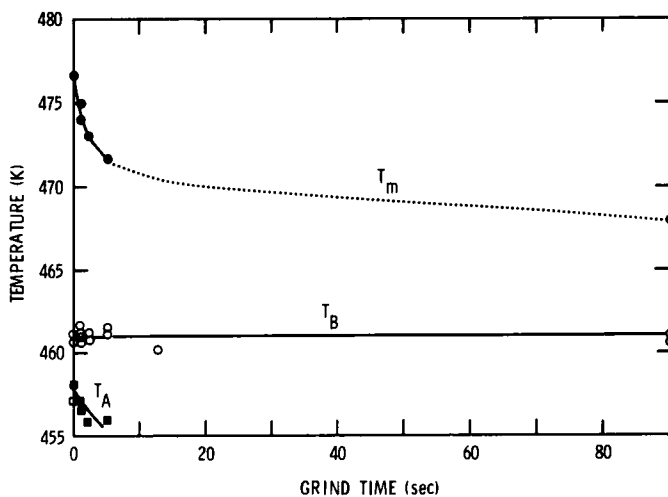


FIGURE 4 Influence of grind time on  $T_A$ ,  $T_B$ , and  $T_m$  the temperatures of the A, B and melting peaks for OPCTS.

with the previous work<sup>5</sup> on heat-treated samples. All support the view that for pure virgin samples nucleation sites are sufficiently rare that long transformation times are observed. Furthermore, as previously reported,<sup>5</sup> the 3-phase can be preserved in small crystallites of a polycrystalline virgin sample for a considerably longer time than in large crystallites. This behavior is consistent with the greater probability of finding a nucleation site in a larger crystallite. On the other hand, heat and mechanical treatments as well as impurities introduce nucleation sites which lead to rapid transformation.

Although calorimetry has previously been used to detect long-term preservation of metastable solid phases in small particles of lithium<sup>19</sup> and organics,<sup>20</sup> these earlier studies did not provide quantitative information on transformation kinetics. The kinetic experiments reported below will quantify the difference in transformation times for small versus large crystallites of OPCTS.

## IV. KINETIC EXPERIMENTS

### A. Samples

As in Reference 5, OPCTS was obtained from a commercial source<sup>21</sup> and was studied without further purification. It is supplied as an atomic absorption standard and is therefore assumed to be of high purity (an assumption which was substantiated by our own purity analysis.)†

Microscopic examination of the crystallites of virgin polycrystalline OPCTS revealed the largest to be  $\geq 1000 \mu\text{m}$  on a side and the smallest  $\leq 50 \mu\text{m}$ . As a first approximation we treat the crystallite size distribution as roughly bimodal. This simplification will help us to interpret the kinetic experiments and is appropriate for two reasons: 1) microscopy (see, for example, Figure 5) showed that about 80% of the mass of a typical 4 mg sample is found in a few ( $\sim 60$ ) large crystals (mesh size  $>150 \mu\text{m}$ ), and 20% in small ones ( $\sim 400$  crystals, mesh size  $<150 \mu\text{m}$ ); 2) the phase transformation kinetics discussed below are governed by two time constants, a short one (which we associate with large crystallites) and a long one (small crystallites). We assume that all virgin samples (weighing a few mg and containing several hundred crystallites) used in our kinetic studies

---

† Calorimetry, mass spectrometry, and gas chromatography measurements indicate purity levels greater than 99.97%.



FIGURE 5 Optical micrograph of virgin OPCTS. The largest crystallites are  $\approx 1000$   $\mu\text{m}$  in length, the smallest  $\approx 50$   $\mu\text{m}$ . From the micrograph we see that it is reasonable to approximate the crystallite size distribution as bimodal (a few large ones, many small ones).

had essentially the same bimodal crystallite distribution. This assumption seemed to be justified by the relative consistency of the kinetic results described below. (Appreciable sample-to-sample skewing of the size distribution would have resulted in enhanced scatter in the  $x$  versus  $t$  plots, due to the dependence of transformation kinetics on crystallite size.)

## B. Experimental procedure

In the kinetic experiments we measured  $L_A$  and  $L_B$  as a function of heat treatment time at a specific "soak" temperature. From Equations (1) and (2) this was equivalent to determining the time-dependence of  $x$  at each soak temperature. The procedure for the experiments was as follows:

1. A sample of pure, virgin OPCTS (weighing from  $\sim 2$  to  $\sim 5$  mg) was prepared, hermetically sealed in an aluminum DSC sample capsule, and weighed according to the procedures of Reference 5.
2. The encapsulated sample was placed in the sample pan of the DSC instrument and covered by the platinum sample cover.<sup>22</sup>

3. The sample temperature was programmed from room temperature to a predetermined soak temperature  $T_s$  at 320 K/min. Since  $T_s$  was always chosen to be near 450 K (i.e., a few degrees below  $T_{31}$ ), the time required to scan to the soak temperature was only about 1/2 minute—usually much less than the time the sample would remain at the soak temperature.

4. The sample was maintained at  $T_s$  for a predetermined time—the soak time  $t_s$ . This time ranged from 0 to 4144 minutes (depending on  $T_s$ ).

5. The sample temperature was then scanned rapidly (in a few seconds) from  $T_s$  to a temperature just below  $T_{31}$ . (This step was unnecessary if  $T_s$  was sufficiently near to  $T_{31}$ .)

6. The temperature was immediately programmed at a standard scan rate (2.5 K/min) through  $T_{31}$  to a temperature several degrees above  $T_{21}$ , allowing both the  $A$  and  $B$  peaks to be recorded and their areas  $L_A$  and  $L_B$  to be determined. The standard scan rate was chosen to be as fast as possible while still allowing both the  $A$  and  $B$  peaks to be fully resolved. (In order to take account of the times required for steps 5 and 6, a small correction time was added to the soak time. The desire to minimize this correction was a motivation for the choice of as fast a standard scan rate as possible.)

Experiments were performed for three different soak temperatures—449 K (175.8°C), 452 K (178.8°C), and 455 K (181.8°C). For each soak temperature a number of virgin OPCTS samples were prepared. For each sample two or more DSC scans through the region of interest were run: the first according to the procedure above, and subsequent one(s) as verification that indeed only a  $B$ -peak was observed (or that only a very small residual  $A$ -peak remained). The subsequent run(s) also permitted a measurement (from  $L_B$ ) of  $L_{21}$  against which the  $L_A$  and  $L_B$  values of the first run could be normalized (i.e., as a check of the sample weight).

### C. Experimental results

The data for  $L_A$  and  $L_B$  (and their sum) for virgin samples as a function of soak time for the three different soak temperatures are plotted in Figures 6 to 8. For each triad of data points ( $L_A$ ,  $L_B$ , and  $L_A + L_B$ ) at a given soak temperature a fresh sample had to be prepared, and thus the experimental determination of the kinetic plots of Figures 6 to 8 was quite time consuming. It is apparent from the figures that the time constant governing the  $3 \rightarrow 2$  transformation is (as expected) faster as soak temperature increases. A surprising as-

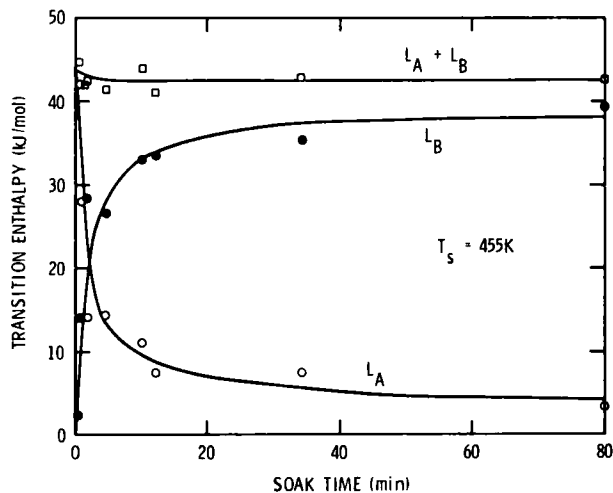


FIGURE 6 Transition enthalpies,  $L_A$ ,  $L_B$ , and  $L_A + L_B$ , of virgin OPCTS versus soak time at a soak temperature of 455 K.

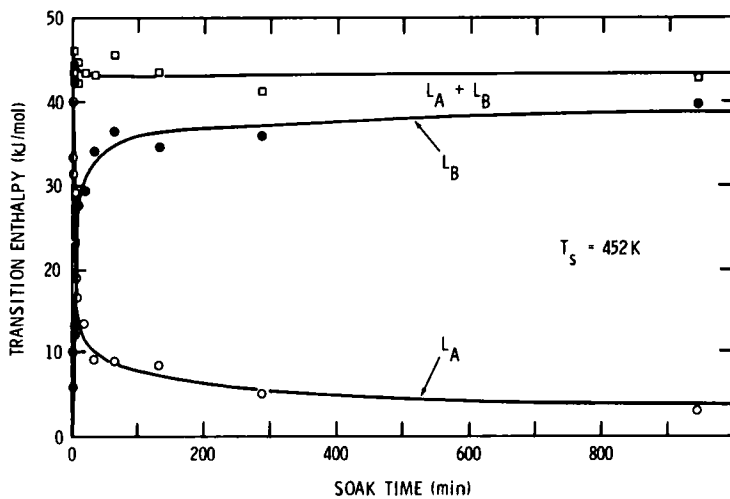


FIGURE 7 Transition enthalpies of virgin OPCTS versus soak time at a soak temperature of 452 K.

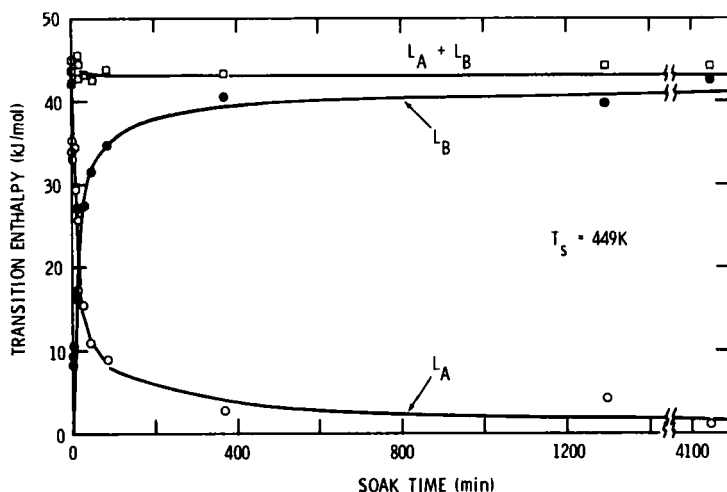


FIGURE 8 Transition enthalpies of virgin OPCTS versus soak time at a soak temperature of 449 K.

pect of the plots is the fact that  $L_A$  was non-zero for the longest soak times chosen, indicating that the metastable phase could be preserved far longer than originally anticipated. The smooth curves of the figures are drawn as an aid to the eye.

## V. ANALYSIS AND INTERPRETATION OF KINETIC EXPERIMENTS

### A. Plots of $x$ versus $t$

From the data of Figures 6 to 8 and Equations (1) and (2) we can determine the dependence of  $x$ , the mole fraction of 3-phase converted to 2-phase, on soak time. Figures 9 to 11 give the results for the three soak temperatures. These three figures may be interpreted as a direct measurement of the kinetics of the  $3 \rightarrow 2$  phase transformation at three different temperatures.

Two aspects of Figures 9 to 11 are apparent. First,  $x$  initially increases very rapidly but subsequently approaches unity very slowly, suggesting that two time constants may be involved. Second, the characteristic times for the curves decrease with increasing temperature as expected.

The need for two time constants to describe each  $x$  versus  $t$  curve is consistent with our assumption of a bimodal crystallite size distri-

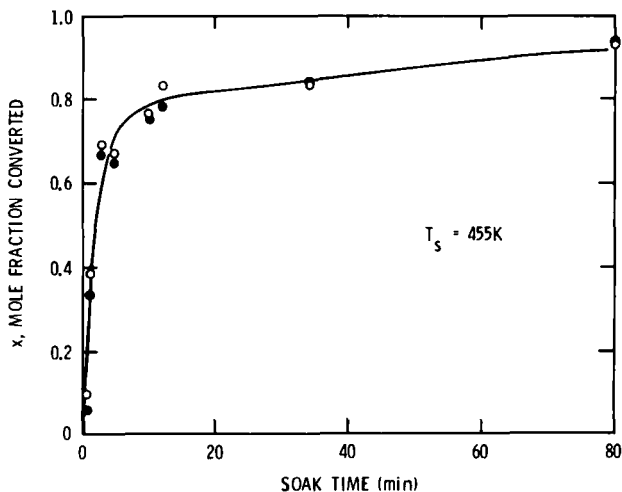


FIGURE 9 Soak-time dependence of  $x$ , the mole fraction of 3-phase converted to 2-phase, for virgin OPCTS at a soak temperature of 455 K. The open circles are values derived from  $L_A$  (Equation 1) the filled circles from  $L_B$  (Equation 2). The curve is a fit of Equation (5) with the values of  $a$ ,  $\tau_1$ , and  $\tau_2$  given in Table I.

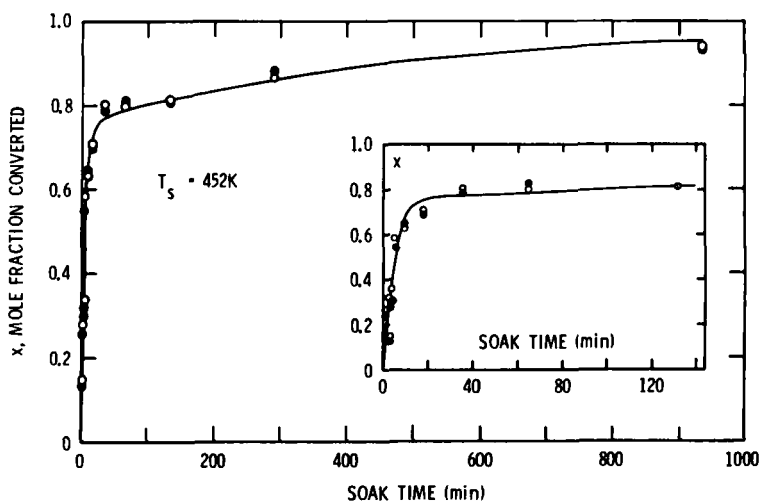


FIGURE 10 Soak-time dependence of  $x$  for virgin OPCTS at a soak temperature of 452 K. The inset shows an expanded time-scale of the plot for shorter times. Symbols as in Figure 8. The curve is a fit of Equation (5) with values of the parameters from Table I.

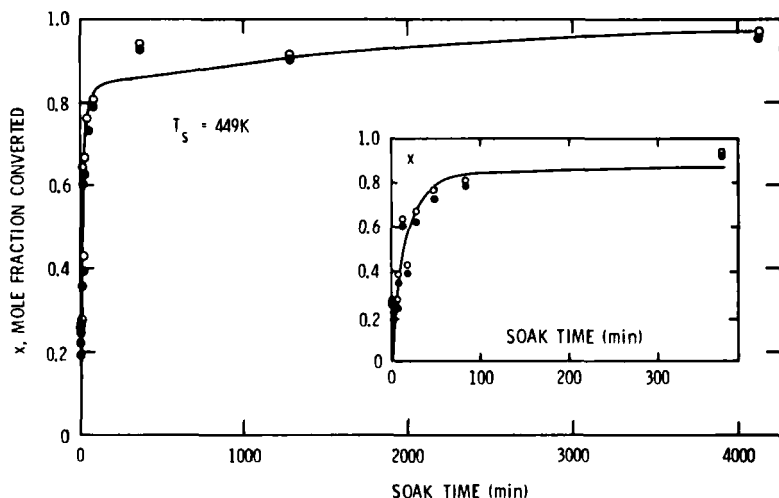


FIGURE 11 Soak-time dependence of  $x$  for virgin OPCTS at a soak temperature of 449 K. The inset shows an expanded time-scale of the plot for shorter times. Symbols as in Figure 8. The curve is a fit of Equation (5) with values of the parameters from Table I.

bution and our observation<sup>5</sup> that large crystallites transform much more rapidly than small ones. Furthermore, the fact that the knee of each curve occurs at around  $x \sim 0.8$  agrees with our determination that approximately 80% of the sample mass is contained in large crystallites.

### B. Model of Cardew, et al.

Cardew, et al.<sup>23</sup> have presented a model for the kinetics of polymorphic solid-state transformations which takes into account both nucleation time  $\tau_N$  and growth time  $\tau_G$ . Their theory stresses the importance of crystal volume,  $V$ , on transformation rate in polycrystalline samples: for bulk nucleation,  $\tau_G/\tau_N$  scales as  $V^{4/3}$ . In the limit where  $\tau_G/\tau_N \rightarrow \infty$  (i.e., transformation kinetics dominated by growth), they obtain the classical Avrami behavior:<sup>24</sup>

$$x = 1 - \exp[-(t/\tau_A)^4] \quad (3)$$

where the time constant  $\tau_A$  is independent of crystallite size. For a nucleation-controlled transformation ( $\tau_G/\tau_N \rightarrow 0$ ), they find

$$x = 1 - \exp(-t/\tau_N), \quad (4)$$



TABLE I

Phase transformation parameters derived from two-exponential fit to DSC soak time experiments

T (K)	<i>a</i>	$\tau_1$ (min)	$\tau_2$ (min)
449	0.83	18.0	2250
452	0.76	4.6	530
455	0.75	1.8	70

where  $\tau_N$  is inversely proportional to crystallite volume.<sup>†</sup>

In Reference 5 it was shown that the linear growth velocity of  $3 \rightarrow 2$  transformation at 436 K is  $\sim 2 \times 10^{-4}$  cm/s. Thus, at that temperature, the largest crystallites would transform from the 3-phase to the 2-phase in a few minutes if the transformation were growth controlled. At soak temperatures of 449 K and above, growth velocities would be considerably higher, and maximum growth times of less than one minute for a typical diffusion-controlled growth would be expected. It is apparent that growth times for the  $3 \rightarrow 2$  transformation are small compared to the time scales of Figures 9–11, so that the phase transformation on this basis would appear to be nucleation-controlled.

Appropriate to the assumed bimodal crystallite size distribution of our virgin OPCTS samples, we approximate the transformation kinetics of a typical polycrystalline sample (composed of several hundred crystallites) by a sum of two expressions like that of Equation (4):

$$x = a[1 - \exp(-t/\tau_1)] + (1-a)[1 - \exp(-t/\tau_2)], \quad (5)$$

where  $\tau_1$  is the short transformation time constant,  $\tau_2$  is the long one, and  $a$  is the mass fraction of material in the large crystallites.<sup>‡</sup>

Equation (5) was fit to the data of Figures 9–11 using a simplex minimization process<sup>25</sup> to derive values of  $a$ ,  $\tau_1$  and  $\tau_2$  for the three soak temperatures. The values derived are given in Table I, and the curves of Figures 9–11 are those calculated from Equation (5), using the parameters of the Table. The  $a$ -values lie in the range  $0.8 \pm 0.05$ ,

<sup>†</sup> The assumption of surface rather than bulk nucleation changes the Cardew model, but  $\tau_N$  still depends on size, scaling as  $S^{-1}$  (where  $S$  is crystal surface area), rather than as  $V^{-1}$ .

<sup>‡</sup> It should be emphasized that Equation (5) is strictly true only for a bimodal distribution consisting of two discrete crystallite sizes. Nevertheless, it is appropriate to use the equation as a first approximation to derive two mean transformation times, rather than to assume a distribution of  $\tau$ -values.

consistent with our previous observation that 80% of each sample's mass is found in large crystallites.

### C. Comparison with nucleation theory

A theory of homogeneous nucleation based on the rate of growth of small nuclei was first put forth by Turnbull and Fisher.<sup>26-28</sup> According to the theory,  $J$ , the nucleation rate per unit volume, is given by

$$J = A \exp[-16\pi\gamma^3 T_0^2 / \{3\lambda^2 (\Delta T)^2 kT\}], \quad (6)$$

where  $A$  is a pre-exponential factor,  $\gamma$  is the interfacial energy between the nucleus of the stable phase and the metastable phase,  $T_0$  is the equilibrium transition temperature ( $= T_{32}$  for OPCTS),  $\lambda$  is the transition enthalpy per unit volume,  $T$  is the temperature,  $\Delta T = T - T_0$ , and  $k$  is the Boltzmann constant.† The pre-exponential factor is given by:

$$A = \frac{NkT}{h} \exp(-\Delta G_f/kT) \quad (7)$$

where  $N$  is the number of molecules per unit volume,  $h$  is the Planck constant, and  $\Delta G_f$  is the Gibbs free energy of activation for transport across the interface between the two phases. Turnbull<sup>27</sup> has argued that most of the temperature dependence of  $J$  is contained in the exponential of Equation (6) and not in the pre-exponential. He verified Equation (6) in a study of the solidification of small droplets of mercury and tin.<sup>27</sup>

The Turnbull-Fisher theory was further substantiated by the work of Taborek<sup>29</sup> who calorimetrically measured the solidification kinetics of supercooled water droplets emulsified in oil. He investigated droplets stabilized using two different surfactants and concluded that in one case the transformation kinetics were controlled by bulk homogeneous nucleation (i.e., nucleation rate scaled with droplet volume). In the second case nucleation was initiated at the droplet surface. In both cases the temperature dependence of the nucleation rate was given by Equation (6). Taborek was able to determine  $\gamma$ , the water/ice interfacial energy from Equation (6), obtaining  $\gamma = 28.3 \text{ ergs/cm}^2$  at 236 K.

---

† It should be pointed out that in the present case  $\Delta T$  is the amount of superheating, in contrast to the supercooling considered by Turnbull and Fisher.

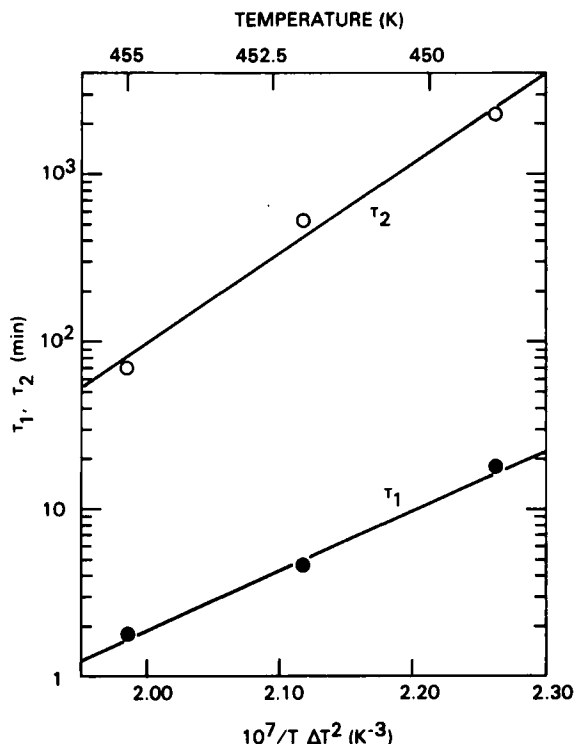


FIGURE 12 Turnbull plot of the data from Table I.

To compare our time-constant results with the nucleation rate expression (Equation (6)) we note, with Turnbull,<sup>27</sup> that

$$J = \frac{1}{V(1-x)} \frac{dx}{dt} = \frac{1}{V\tau_N} \quad (8)$$

where  $V$  is the mean crystallite volume and  $\tau_N$  is the nucleation time constant of Equation (4). We equate the two expressions (6) and (8) for  $J$  and note that, if the  $3 \rightarrow 2$  transformation in virgin polycrystalline OPCTS samples is nucleation-controlled, semilogarithmic plots of  $\tau_1$  (large crystallite nucleation time) and  $\tau_2$  (small crystallite nucleation time) versus  $(T \Delta T^2)^{-1}$  should yield straight lines. The appropriate plots are given in Figure 12; a linear dependence is indicated in each case.<sup>†</sup>

<sup>†</sup> Although only three data points each are given for  $\tau_1$  and  $\tau_2$ , we note that only four points were given in the original paper of Turnbull.<sup>27</sup> The paucity of data is, of course, due to the extremely time-consuming nature of the experiments.

The slopes of the two lines of Figure 12 should, from Equation (6), be proportional to  $1/\lambda^2$ . The fact that the slope of the  $\tau_2$  curve is greater than that for  $\tau_1$  suggests that the transition enthalpy for smaller crystallites is slightly smaller than that for the larger ones. This is consistent with observations<sup>30-32</sup> that transition temperatures decrease with decreasing sample volume, undoubtedly due to the enhanced contribution of material transforming at the surface.<sup>33</sup>

It is possible to make a rough estimate of  $\gamma_{32}$ , the interfacial energy between the 3- and 2-phases in the manner of Turnbull<sup>27</sup> and Tabor<sup>29</sup> using the full Turnbull-Fisher expression, Equations (6) and (7), and an estimate of  $J$  from Equation (8). The value of  $\lambda$  is<sup>5</sup>

$$\lambda = L_{32} \approx 3 \text{ KJ/mole} = 4.5 \times 10^7 \text{ ergs/cm}^3$$

For the large OPCTS crystallites, we estimate  $V \approx (5 \times 10^{-2})^3 = 1.3 \times 10^{-4} \text{ cm}^3$  and  $\tau_1 \approx 10^3 \text{ s}$  at  $T = 449 \text{ K}$ . Thus, the only unknown quantity needed for the evaluation of  $\gamma_{32}$  is  $\Delta G_f$ . However, as is readily seen by inspection of the Turnbull-Fisher expression, the value of  $\gamma$  is not at all sensitive to the value of  $\exp(-\Delta G_f/kT)$ . In fact, for a range of the exponential from  $2 \times 10^{-1}$  to  $4 \times 10^{-8}$  (selected from the values used by Turnbull and Tabor and from the diffusional activation energy for OPCTS in the 1-phase<sup>13</sup>), we calculate that  $\gamma_{32}$  ranges from 3.25 to 3.51 ergs/cm<sup>2</sup>.† Thus, as anticipated in Section II,  $\gamma_{32}$ , the interfacial energy between the 3- and 2-phases is fairly small, about an order of magnitude less than that for a liquid-solid interface.

We are now able to estimate  $r_c$ , the radius of a critical nucleus of 2-phase, at 449 K according to the relation<sup>28,29</sup>

$$r_c \approx \frac{2\gamma T_0}{\lambda \Delta T} \quad (9)$$

The critical nucleus of 2-phase in 3-phase at 449 K has a radius of 52 Å and contains approximately 540 molecules. At lower temperatures (closer to  $T_0 = T_{32}$ ) the critical radius would be still larger: assuming  $\gamma$  and  $\lambda$  are constant, we calculate that at 360 K (just above  $T_{32}$ ),  $r_c$  would be roughly 500 Å, and the nucleus would contain  $\sim 10^4$  molecules. The difficulty in creating such a large nucleus and hence in

† The insensitivity of  $\gamma$  to  $\exp(-\Delta G_f/kT)$  is due to the facts that  $NkT/h$  is very large ( $\sim 10^{34}$ ) and that  $\gamma$  occurs as a cubic in an exponential.

TABLE II  
Nominal crystallite sizes

Mesh size (μm)	Surface area (cm <sup>2</sup> ) <sup>a</sup>			Volume (cm <sup>3</sup> ) <sup>a</sup>		
	Min	Max	Mean	Min	Max	Mean
>425	$2.3 \times 10^{-2}$	$6.4 \times 10^{-2}$	$(3.2 \pm 1.2) \times 10^{-2}$	$2.6 \times 10^{-4}$	$11.1 \times 10^{-4}$	$(4.4 \pm 2.6) \times 10^{-4}$
<425, >250	$3.6 \times 10^{-3}$	$22.7 \times 10^{-3}$	$(9.8 \pm 4.6) \times 10^{-3}$	$1.7 \times 10^{-5}$	$22.8 \times 10^{-5}$	$(7.7 \pm 5.3) \times 10^{-5}$
<250, >150	$2.3 \times 10^{-3}$	$6.4 \times 10^{-3}$	$(4.4 \pm 1.2) \times 10^{-3}$	$8.1 \times 10^{-6}$	$36.0 \times 10^{-6}$	$(22.2 \pm 8.8) \times 10^{-6}$
<150, >75	$2.5 \times 10^{-4}$	$29.4 \times 10^{-4}$	$(9.9 \pm 6.7) \times 10^{-4}$	$0.31 \times 10^{-6}$	$11.0 \times 10^{-6}$	$(2.6 \pm 2.6) \times 10^{-6}$
<75	$2.2 \times 10^{-4}$	$6.1 \times 10^{-4}$	$(3.8 \pm 1.0) \times 10^{-4}$	$0.25 \times 10^{-6}$	$1.1 \times 10^{-6}$	$(0.57 \pm 0.22) \times 10^{-6}$

<sup>a</sup>Crystallite surface areas and volumes were calculated from optical microphotographs assuming cylindrical crystal shapes.

nucleating the stable 2-phase would explain the ability to preserve the metastable 3-phase above  $T_{32}$  in virgin samples.

## VI. EFFECT OF CRYSTALLITE SIZE

In the above discussion based on the model of Carew, et al., we considered the  $3 \rightarrow 2$  phase transformation kinetics to be governed by bulk nucleation, for which  $\tau_N \sim 1/V$ . However, the possibility that nuclei are initiated at crystal faces should not be ruled out, in which case  $\tau_N \sim 1/S$ , where  $S$  is the crystallite surface area. Therefore, it is important to determine the  $3 \rightarrow 2$  phase transformation time constant as a function of crystal size for two reasons: 1) to verify quantitatively our previous<sup>5</sup> qualitative determination that the phase transformation is faster for larger crystals; and 2) to determine whether the transformation time  $\tau$  varies as  $1/V$  or  $1/S$  to assess whether nucleation is bulk- or surface-induced.

### A. Sample preparation

To determine the size dependence of  $\tau$ , we separated crystals into five size "classes" using four standard meshes (425  $\mu\text{m}$ , 250  $\mu\text{m}$ , 150  $\mu\text{m}$ , and 75  $\mu\text{m}$ ). The nominal size ranges of each class are shown in column 1 of Table II. The crystallites in the various size ranges were roughly cylindrical in shape. (However, a greater departure from cylindrical shape was noted for smaller crystallites.) The dimensions of a number of crystallites for each size range were determined, and minimum, maximum, and mean surface areas and volumes for each size range were calculated under the assumption of cylindrical shape (an assumption which becomes less appropriate for smaller crystallites). These area and volume values are also shown in Table II. It is evident that both area and volume vary appreciably within each size range. Nevertheless, the size range of each of the five size classes is sufficiently narrow that reasonable size-dependent trends should be discernible.

### B. DSC experiments

Two samples from each size class were encapsulated for DSC study (sample masses are shown in Table III). The number of crystallites in a given sample ranged from 10 to 15 for large crystallites to several thousand for the smallest crystallites. The DSC data were taken in a manner similar to that described in Section IV-B above. The tem-

TABLE III

Influence of crystallite size on mole fraction transformed and transformation time constants for virgin OPCTS samples

Mesh size ( $\mu\text{m}$ )	Sample mass (mg)	$x_A$	$x_B$	$\tau_A$ (min)	$\tau_B$ (min)
>425	4.70	0.980	0.985	0.805	0.750
	5.46	0.925	0.912	1.12	1.20
<425, >250	5.37	0.443	0.427	5.01	5.26
	6.16	0.508	0.483	4.23	4.55
<250, >150	3.75	0.270	0.276	9.85	9.60
	4.47	0.234	0.243	10.69	10.24
<150, >75	3.47	0.108	0.126	24.50	20.79
	3.24	0.0936	0.105	29.31	25.96
<75	3.13	0.070	0.078	38.9	34.72
	4.27	0.079	0.094	34.8	28.97

perature of each virgin sample was scanned at 320 K/min to 452 K and then immediately programmed through the *A*- and *B*-peaks at 2.5 K/min. The “soak time,”  $\Delta t$ , for each experiment was taken to be the total elapsed time before the onset of the *A*-peak (nominally  $\sim 3$  minutes). The determination of the  $\Delta t$  value was not critical since the soak time was essentially the same for all virgin runs. Furthermore, we are mainly interested in the *relative* values of transformation time as a function of crystallite size.

After each virgin sample DSC run, the sample was melted and then cooled to 380 K where it was allowed to solidify. A subsequent DSC run allowed us to determine  $L_{21}$  from the area of the *B*-peak.<sup>†</sup> This determination of  $L_{21}$  enabled us to make a small correction to the virgin sample values of  $L_A$  and  $L_B$ , if needed, to compensate for small errors in measurement of sample mass. The corrections were always small ( $\leq \pm 1\%$ ).

### C. Analysis of DSC results

As before, values of  $x$ , the mole fraction of virgin sample 3-phase which converted to 2-phase during the soak time  $\Delta t$ , were determined from the *A*- and *B*-peaks using Equations (1) and (2). The resulting magnitudes,  $x_A$  and  $x_B$ , are given in columns 3 and 4 of Table III. The corresponding values of the time constant for  $3 \rightarrow 2$  transfor-

<sup>†</sup> As mentioned earlier (Section IV.B and Reference 5) no *A*-peak is found for previously melted samples. Thus for this case,  $L_B = L_{21}$  since  $x = 1$  in Equation (2).

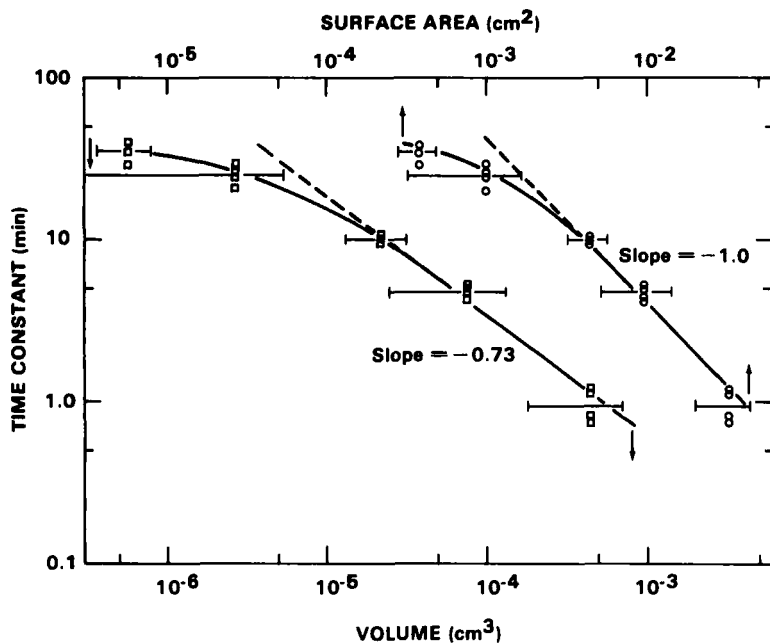


FIGURE 13 Log-log plot of time constant,  $\tau$ , (from Table III) versus mean crystallite volume ( $\square$ ) and mean crystallite surface area ( $\circ$ ) (from Table II). The error bars indicate the standard deviations of mean crystallite volume and area.

mation,  $\tau_A$  and  $\tau_B$ , could then be determined by inverting Equation (4):†

$$\tau = -\Delta t / \ln(1 - x). \quad (10)$$

The resulting values,  $\tau_A$  and  $\tau_B$ , for each sample are also given in Table III.

#### D. Results

It is apparent from Table III that the transformation time constant  $\tau$  is strongly dependent on crystallite size, thus further strengthening our contention that nucleation controls the transformation kinetics.

To determine whether nucleation occurs in the bulk or at the surface, we plot, in Figure 13,  $\ln \tau$  versus  $\ln V$  and  $\ln S$ . It is apparent

† We assumed that the size distribution in each size class was sufficiently narrow that the transformation kinetics were governed by a single time constant, an assumption which, of course, fails in direct relation to the breadth of the size distribution for that class.



that, at least for larger crystallites  $\tau \sim 1/S$ , suggesting that nucleation does occur at crystallite surfaces. The departure of the plot from linearity for smaller crystallites is not fully understood, but is probably due to the greater departure from cylindrical shape for the smallest crystallites. Indeed, the smallest crystallites are so irregular† that their true surface areas are likely to be considerably larger than the values estimated from the cylindrical approximation. A correction for this underestimation of surface area would increase the  $S$ -values for the smallest crystallites and tend to bring the corresponding  $\tau$  results into better agreement with the  $1/S$  dependence in Figure 13.

The assumption of a single transformation time constant for each size class is also a source of discrepancy, especially for small crystallites, due to the greater sensitivity to small values of  $S$  (or  $V$ ). Thus the  $\tau$ -value for each class is not a true time constant for a single exponential transformation process, but is some sort of average over a size distribution of limited range. Furthermore, since the experimental  $\Delta t$  value was only  $\sim 3$  minutes, the measured  $\tau$ -values are characteristic of the initial stages of the  $3 \rightarrow 2$  transformation process.

In spite of these limitations on our estimates of both  $S$  and  $\tau$ , we feel that the size dependent studies are very instructive in that they further confirm the view that nucleation controls the  $3 \rightarrow 2$  transformation rate in virgin samples and that the nucleation sites are more likely found at surfaces than in the bulk.

## VII. CONCLUSIONS

In this paper we have demonstrated four things:

1. It is possible to use differential scanning calorimetry (DSC) to measure phase transition kinetics of sluggish solid-solid transformations. (Time-dependent effects have been observed previously,<sup>5,11,19,20</sup> but direct kinetic data were not obtained in those studies.)
2. The  $3 \rightarrow 2$  transformation in superheated virgin polycrystalline samples of OPCTS is nucleation controlled. The evidence for this conclusion is multifold: a) the sluggishness of the transformation in virgin samples; b) the rapidity of transformation in heat treated, ground or impure samples; c) the rapidity of crystal growth rate

---

†The departure from cylindrical shape can be seen in Figure 2 of Reference 5 and Figure 5 of the present work. The fact that in the present Figure 13  $\tau$  for large crystallites goes as  $V^{-0.73}$  and  $S^{-1}$  rather than  $V^{-2/3}$  and  $S^{-1}$  is a further indication of the crudeness of the cylindrical shape approximation.

compared to total transformation rate; d) the agreement of the temperature dependence of transformation times with Turnbull-Fisher nucleation theory; and e) the dependence of transformation times on crystallite size. The fact that transformation time scales more closely with the inverse of crystallite area than with the inverse of volume suggests that nucleation is initiated at the crystal surface.

3. The temperature dependence of the nucleation times suggests that the latent heats of small crystallites may be slightly smaller than that of the bulk (i.e., large crystallites).

4. From the Turnbull-Fisher theory,  $\gamma_{32}$ , the interfacial energy between the 3 and 2 phases of OPCTS, has been estimated. The value obtained,  $\sim 3.3$  ergs/cm<sup>2</sup>, is an order of magnitude smaller than that for a liquid-solid interface. This result is not unreasonable in view of the assumed small difference in Gibbs free energy between the two phases.

### Acknowledgments

The author thanks J. G. Gay, J. P. Hirth, J. Billard, and J. R. Bradley for valuable discussions, and P. Taborek for making his results available prior to publication. He also thanks J. G. Gay for performing the simplex minimization calculation, J. C. Price for computational assistance, and K. L. Olson for mass spectrometric and gas chromatographic studies of sample purity.

### ADDENDUM

Recently, Sambles<sup>34</sup> presented a detailed equilibrium thermodynamic treatment of the effect of particle size on first-order solid-solid phase transformations. He developed an expression for the depression (or increase) of transition temperature in terms of the density, surface energy, crystallite dimension, molecular weight, and entropy of transition. He pointed out that, for a solid-solid transformation in a small perfect crystal, nucleation must occur at the surface, and furthermore, that there is no reason why perfect crystals should not substantially *superheat* as well as *supercool* at their first-order phase transitions.

### NOTE ADDED IN PROOF

J. P. Hirth has pointed out (private communication) that it is also possible to explain the slope differences of the  $\tau_1$  and  $\tau_2$  curves in Figure 12 by an increase in  $\gamma$  with decreasing crystal size rather than by a decrease in  $\lambda$  (see Equation 6). Thus, either an 18% decrease

in  $\lambda$  (from  $\sim 3$  KJ/mol. to 2.5 KJ/mol.) or a 14% increase in  $\gamma$  (from  $\sim 3.3$  ergs/cm<sup>2</sup> to  $\sim 3.77$  ergs/cm<sup>2</sup>) would explain the slope difference.

It should also be mentioned that the low value of interfacial energy between the 3 and 2 phases is apparently associated with a very small volumetric change between the two phases. The data of Hyde, et al.<sup>7</sup> (the only x-ray crystallographers who studied both low temperature phases) shows only a 0.3% volume expansion on going from the monoclinic structure (stable at room temperature<sup>9</sup>) to the triclinic.

## References

1. J. D. Brooks and G. H. Taylor, *Chem. Phys. of Carbon*, **4**, 243 (1968); J. Dubois, C. Agache and J. L. White, *Metallog.* **3**, 337 (1970).
2. See, for example, J. B. Zeldovich, *Acta Physicochim. U.R.S.S.*, **18**, 1 (1943); A. Kantrowitz, *J. Chem. Phys.*, **19**, 1097 (1951); D. Turnbull, *Solid State Phys.*, **3**, 225 (1956); K. C. Russell, in "Phase Transformations," Am. Soc. for Metals, Metals Park, Ohio (1970), p. 219; M. E. Fine, "Phase Transformations in Condensed Systems," MacMillan, New York (1964); P. T. Cardew, R. J. Davey, and A. J. Ruddick, *J. Chem. Soc., Faraday Trans. 2*, **80**, 659 (1984).
3. W. C. McCrone, in "Physics and Chemistry of the Organic Solid State," Vol. 2, D. Fox, M. M. Labes and A. Weissberger (eds.), Interscience, New York (1965), p. 725.
4. J. W. Mullin, "Crystallization," Butterworth and Co., London (1972), p. 137.
5. G. W. Smith, *Phase Transitions*, **1**, 107 (1979).
6. C. A. Burkhard, B. F. Decker and D. Harker, *J. Am. Chem. Soc.*, **67**, 2173 (1945).
7. J. F. Hyde, L. K. Frevel, H. S. Nutting, P. S. Petrie and M. A. Purcell, *J. Am. Chem. Soc.*, **69**, 488 (1947).
8. M. A. Hossain, M. B. Hursthouse and K. M. A. Malik, *Acta Cryst.*, **B35**, 522 (1979).
9. D. Braga and G. Zanotti, *Acta Cryst.*, **B36**, 950 (1980).
10. P. H. Keyes and W. B. Daniels, *J. Chem. Phys.*, **105**, 484 (1975).
11. B. Dubini, S. Melone, M. G. Ponzi-Bossi and F. Rustichelli, in "Advances in Liquid Crystal Research and Applications," L. Bata (ed.), Pergamon Press, Oxford (1980), p. 179.
12. G. Albertini, B. Dubini, S. Melone, F. Rustichelli and G. Torquati, in "Liquid Crystals of One- and Two-Dimensional Order," W. Helfrich and G. Heppke (eds.), Springer-Verlag, Berlin (1980), p. 53.
13. A. R. Britcher, Ph.D. Thesis, University of Kent, Canterbury (1978).
14. T. C. Moore, Ph.D. Thesis, University of Texas, Austin (1981). (Unfortunately, this work contains several misinterpretations of the results of Reference 5, including a significant misstatement of the values of  $L_{31}$  and  $L_{21}$  in Table V-2 of the thesis.)
15. M. Bée, A. J. Dianoux and F. Volino, *Mole. Phys.*, **51**, 24 (1984).
16. V. Raghavan and M. Cohen, in "Treatise on Solid State Chemistry, Vol. 5, Changes of State," N. B. Hannay (ed.), Plenum, New York (1975), p. 67. See also L. A. Tarshis, J. L. Walker, M. F. X. Gigliotti, *Ann. Rev. Mat. Sci.*, **2**, 181 (1972).
17. See, for example, D. Turnbull, *Trans. AIMME*, **175**, 774 (1948); J. W. Mullin (loc. cit.), p. 146; L. A. Tarshis, et al. (loc. cit.), p. 183; J. L. Katz and M. D. Donohue, *Adv. Chem. Phys.*, **40**, 137 (1979).
18. Wig-L-Bug, Crescent Dental Mfg. Co., Chicago, IL.

19. M. Lambert, Ch. Mazieres and A. Guinier, *J. Phys. Chem. Solids*, **18**, 129 (1961); C. Taupin, M. Lambert and Ch. Maziers, *J. Phys. Chem. Solids*, **32**, 2045 (1971).
20. J. P. Dumas, *J. Phys. C: Solid State Phys.*, **12**, 2225 (1979).
21. Eastman Organic Chemicals, Rochester, NY.
22. Perkin-Elmer Model DSC-2 differential scanning calorimeter, Perkin-Elmer Corp., Norwalk, CT.
23. P. T. Cardew, R. J. Davey and A. J. Ruddick, *J. Chem. Soc.*, Faraday Trans. 2, **80**, 659 (1984); and in "Powtech 83: Particle Technology—(Symposium Series: The Institute of Chemical Engineers, No. 69)," Pergamon Press, Oxford (1983), p. 123.
24. M. Avrami, *J. Chem. Phys.*, **7**, 1103 (1939); *J. Chem. Phys.*, **8**, 212 (1940), *J. Chem. Phys.*, **9**, 177 (1941).
25. J. A. Nelder and R. A. Mead, *Comp. J.*, **7**, 308 (1965).
26. D. Turnbull and J. C. Fisher, *J. Chem. Phys.*, **17**, 71 (1949).
27. D. Turnbull, *J. Chem. Phys.*, **18**, 768 (1950).
28. J. W. Mullin, loc. cit., p. 143ff.
29. P. Taborek, private communication (submitted to Physical Review).
30. D. Armitage and F. P. Price, *Chem. Phys. Letters*, **44**, 305 (1976).
31. P. R. Couchman and W. A. Jesser, *Nature*, **269**, 481 (1977).
32. V. P. Skvipov, V. P. Koverda and V. N. Skokov, *Phys. Stat. Solidi (a)* **66**, 109 (1981).
33. J. W. M. Frenken and J. F. VanderVeen, *Phys. Rev. Letters*, **54**, 134 (1985).
34. J. R. Sambles, *J. Phys. Chem. Solids*, **46**, 525 (1985).